

A study of the relaxation mechanism of a $\text{KAl}(\text{SO}_4)_2 \cdot 12\text{H}_2\text{O}$ single crystal by observation of its ^{39}K and ^{27}Al spin–lattice relaxation processes

This article has been downloaded from IOPscience. Please scroll down to see the full text article.

2004 J. Phys.: Condens. Matter 16 4403

(<http://iopscience.iop.org/0953-8984/16/25/001>)

View [the table of contents for this issue](#), or go to the [journal homepage](#) for more

Download details:

IP Address: 129.252.86.83

The article was downloaded on 27/05/2010 at 15:36

Please note that [terms and conditions apply](#).

A study of the relaxation mechanism of a $\text{KAl}(\text{SO}_4)_2 \cdot 12\text{H}_2\text{O}$ single crystal by observation of its ^{39}K and ^{27}Al spin–lattice relaxation processes

Ae Ran Lim^{1,3} and Se-Young Jeong²

¹ Department of Physics, Jeonju University, Jeonju 560-759, Korea

² Department of Physics, Pusan National University, Pusan 609-735, Korea

E-mail: aeranlim@hanmail.net and ARL29@cornell.edu

Received 6 March 2004

Published 11 June 2004

Online at stacks.iop.org/JPhysCM/16/4403

doi:10.1088/0953-8984/16/25/001

Abstract

The spin–lattice relaxation processes of the ^{39}K and ^{27}Al nuclei in $\text{KAl}(\text{SO}_4)_2 \cdot 12\text{H}_2\text{O}$ crystals were studied; we found that these processes can be described by linear combinations of two and three exponential functions, respectively. From these results, we conclude that the discontinuity in the curve of the spin–lattice relaxation rate near T_c ($=360$ K) corresponds to the first-order phase transition of the crystal. In the case of the ^{39}K nucleus, the relaxation rate increases as the temperature increases. The relaxation rate of the ^{27}Al nucleus decreases below T_c as the temperature increase, while above T_c its relaxation rate increases with increasing temperature. The temperature dependences of these spin–lattice relaxation rates can be described with the power law $T_1^{-1} \propto T^k$. Least square fits of the relaxation rates at temperatures below T_c indicate that $k = 2$ for the ^{39}K nucleus and $k = 7$ for the ^{27}Al nucleus. From these results, we conclude that the ^{39}K and ^{27}Al spin–lattice relaxations occur from Raman relaxation processes.

1. Introduction

The crystallization of $\text{KAl}(\text{SO}_4)_2 \cdot 12\text{H}_2\text{O}$ from aqueous solution has been widely studied not only because $\text{KAl}(\text{SO}_4)_2 \cdot 12\text{H}_2\text{O}$ is an important material in the chemical industry, but also because it is easy to work with in the laboratory, making it a good model system for studying crystallization. Researchers have investigated the solution structures of $\text{KAl}(\text{SO}_4)_2 \cdot 12\text{H}_2\text{O}$ in many supersaturated solutions using a variety of experimental techniques [1–5].

The room temperature structure of $\text{KAl}(\text{SO}_4)_2 \cdot 12\text{H}_2\text{O}$ has been determined using x-ray diffraction [6]. $\text{KAl}(\text{SO}_4)_2 \cdot 12\text{H}_2\text{O}$ single crystals have a cubic structure and belong to the space

³ Author to whom any correspondence should be addressed.

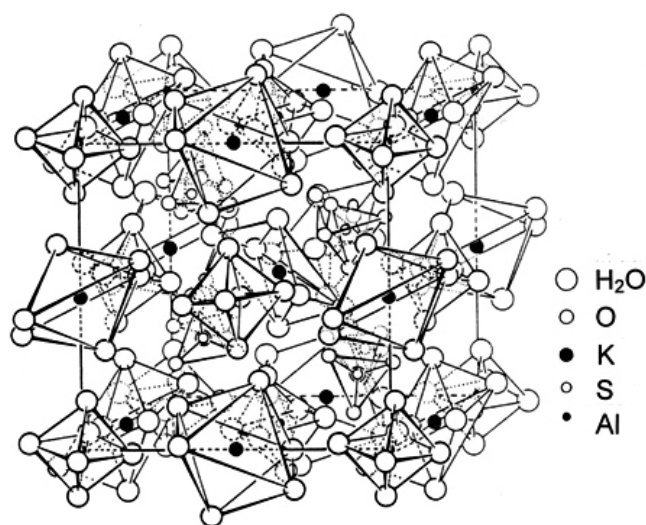


Figure 1. The cubic structure of a $\text{KAl}(\text{SO}_4)_2 \cdot 12\text{H}_2\text{O}$ single crystal at room temperature.

group $Pa\bar{3}$ (point group $m\bar{3}$), with four molecules per unit cell [7]. The lattice parameters of this cubic structure are $a = b = c = 12.157 \text{ \AA}$ at room temperature. The ^{39}K and ^{27}Al metal ions in the $\text{KAl}(\text{SO}_4)_2 \cdot 12\text{H}_2\text{O}$ crystal are each surrounded by six water molecules, as shown in figure 1. The six water molecules that surround the trivalent cation form a nearly regular octahedron. The Al–W(2) distance is 1.908 \AA , whereas the K–W(1) distance has a mean value of 2.983 \AA , where W(2) and W(1) are the oxygen atoms of the water molecules around Al and K, respectively [8]. However, the octahedron formed by the six water molecules around the monovalent cation is significantly distorted by compression along the threefold axis of the crystal.

Until now, the phase transition temperature of $\text{KAl}(\text{SO}_4)_2 \cdot 12\text{H}_2\text{O}$ crystals has not been exactly established. According to Gronvold and Meisingset [9], the enthalpy of transition of $\text{KAl}(\text{SO}_4)_2 \cdot 12\text{H}_2\text{O}$ to $\text{KAl}(\text{SO}_4)_2 \cdot 3\text{H}_2\text{O}$ plus aqueous solution at 358.99 K is 95.2 kJ mol^{-1} . Burns [10] reported that the phase transition in $\text{KAl}(\text{SO}_4)_2 \cdot 12\text{H}_2\text{O}$ was observed at 98 K . The paramagnetic resonance of a polycrystalline sample of $\text{KAl}(\text{SO}_4)_2 \cdot 12\text{H}_2\text{O}$ was first observed by Pake [11]. Bloembergen [12] studied the spin–lattice relaxation time T_1 for the proton resonance in $\text{KAl}(\text{SO}_4)_2 \cdot 12\text{H}_2\text{O}$, containing different amounts of Cr^{3+} , as a function of temperature. In addition, the complete resolution of both the $(1/2, 3/2)$ and $(3/2, 5/2)$ transitions of the ^{27}Al nuclei in a mixture of potassium and ammonium alums [$\text{KAl}(\text{SO}_4)_2 \cdot 12\text{H}_2\text{O}$ and $\text{NH}_4\text{Al}(\text{SO}_4)_2 \cdot 12\text{H}_2\text{O}$] has been reported by Oldfield *et al* [13]. Although the crystal morphology and kinetics of crystal growth of $\text{KAl}(\text{SO}_4)_2 \cdot 12\text{H}_2\text{O}$ have been studied extensively [14–16], sufficient research has not yet been conducted into its nuclear magnetic resonance (NMR) characteristics.

In order to obtain information about the phase transition and the nature of the relaxation processes in a $\text{KAl}(\text{SO}_4)_2 \cdot 12\text{H}_2\text{O}$ single crystal, it is necessary to measure its spin–lattice relaxation time, T_1 . In this paper, the temperature dependences of T_1 for the ^{39}K and ^{27}Al nuclei in a $\text{KAl}(\text{SO}_4)_2 \cdot 12\text{H}_2\text{O}$ single crystal grown using the slow evaporation method were investigated using a pulse NMR spectrometer. The correlation of the Raman process with the ^{39}K and ^{27}Al spin–lattice relaxations is a new result, and is discussed in this paper in the context of the mechanism of the phase transition.

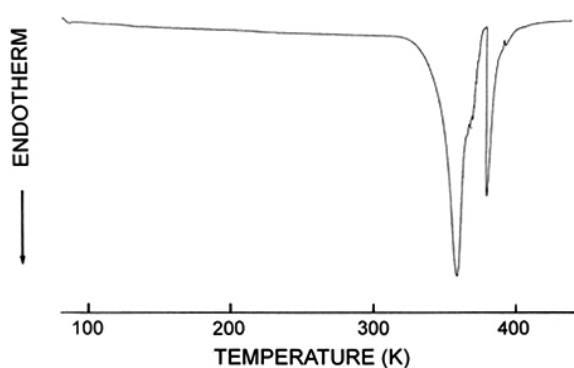


Figure 2. The differential scanning calorimetry thermogram of a $\text{KAl}(\text{SO}_4)_2 \cdot 12\text{H}_2\text{O}$ single crystal.

2. Experimental method

Crystals of $\text{KAl}(\text{SO}_4)_2 \cdot 12\text{H}_2\text{O}$ were grown from water solution. A four-sided face usually formed along the (011) direction and sometimes also along the (001) direction. The faces were easily identified from the crystal morphology and also from Laue x-ray photographs. The $\text{KAl}(\text{SO}_4)_2 \cdot 12\text{H}_2\text{O}$ specimens were prepared in the form of rectangular parallelepipeds with dimensions of $5 \times 5 \times 3 \text{ mm}^3$ from large single crystals of high optical quality grown from aqueous solutions by controlled evaporation at 315 K.

The nuclear magnetic resonance signals of ^{39}K and ^{27}Al nuclei in the $\text{KAl}(\text{SO}_4)_2 \cdot 12\text{H}_2\text{O}$ single crystal were measured using Varian INOVA 600 FT NMR and Bruker DSX 400 FT NMR spectrometers, respectively, at the Korea Basic Science Institute. The static magnetic fields were 14.1 and 9.4 T, and the central radio frequency was set at $\omega_0/2\pi = 27.99 \text{ MHz}$ for the ^{39}K nucleus and at $\omega_0/2\pi = 104.23 \text{ MHz}$ for the ^{27}Al nucleus. The line-width for ^{39}K and ^{27}Al nuclei at 200 K was 0.51 and 8.93 kHz, respectively. The spin–lattice relaxation time was measured by applying a pulse sequence of $\pi-t-\pi/2$. The nuclear magnetizations $S(t)$ of ^{39}K and ^{27}Al nuclei at time t after the π pulse were determined from the inversion recovery sequence following the pulse. The width of the π pulse was $30 \mu\text{s}$ for ^{39}K and $14 \mu\text{s}$ for ^{27}Al , respectively. The temperature dependence of the spin–lattice relaxation time, T_1 , was studied in the range 160–400 K. The sample temperature was stabilized within 0.5 K by controlling the current to a heater. The heater was placed in either a dry air or cold nitrogen gas flow from a liquid Dewar, depending on the temperature range.

3. Experimental results and analysis

To determine the phase transition temperature, differential scanning calorimetry (DSC) was carried out on the crystals using a DuPont 2010 DSC instrument. Measurements were made at a heating rate of 5 K min^{-1} . Endothermic peaks were observed at 358 and 378 K, as shown in figure 2. The first peak corresponds to the phase transition, and the second peak corresponds to the melting of the crystal. This phase transition temperature of 358 K is consistent with the suggestion of Gronvold and Meisingset [9].

The central radio frequency was fixed at 27.99 MHz, which is the Larmor frequency of the ^{39}K nucleus in an applied magnetic field of 14.1 T. When the crystal is rotated about its crystallographic axis, crystallographically equivalent nuclei are expected to give rise to three

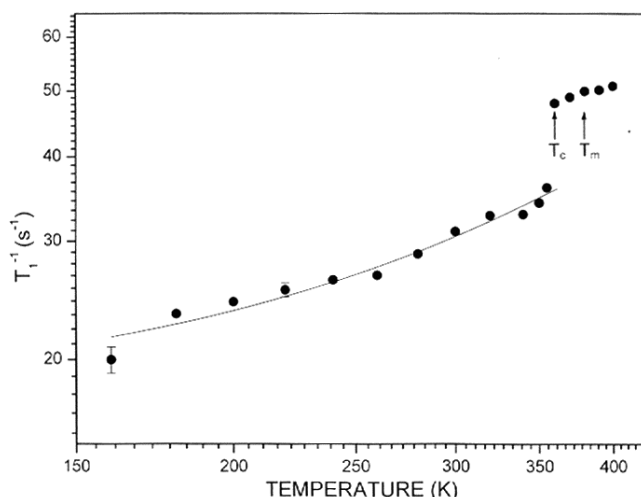


Figure 3. Temperature dependence of the spin–lattice relaxation rate, T_1^{-1} , of ^{39}K nuclei in a $\text{KAl}(\text{SO}_4)_2 \cdot 12\text{H}_2\text{O}$ single crystal.

lines in the NMR spectrum: one central line and two satellite lines. Only one resonance line is obtained for ^{39}K in the case of the $\text{KAl}(\text{SO}_4)_2 \cdot 12\text{H}_2\text{O}$ crystal, which indicates that it has a cubic structure. In a cubic crystal, the electric quadrupole moments of the ^{39}K nucleus cause no perturbation of the four nuclear Zeeman levels, so all transitions contribute to a single resonance line. For the ^{39}K nucleus, the spin–lattice relaxation mechanism is magnetic. The spin–lattice relaxation times of ^{39}K ($I = 3/2$, natural abundance 93.1%) in the $\text{KAl}(\text{SO}_4)_2 \cdot 12\text{H}_2\text{O}$ crystal were measured over the temperature range 160–400 K. The spin–lattice relaxation times were measured using the inversion recovery method. The recovery trace for the single resonance line of ^{39}K with magnetic effects can be represented by a linear combination of two exponential functions [17]:

$$[S(\infty) - S(t)]/2S(\infty) = [0.1 \exp(-2Wt) + 0.9 \exp(-12Wt)] \quad (1)$$

where $S(t)$ is the nuclear magnetization at time t after saturation, and the relaxation time is given by

$$1/T_1 = 2W. \quad (2)$$

We measured the variation of the relaxation time for ^{39}K with temperature. The temperature dependence of the nuclear spin–lattice relaxation rate, T_1^{-1} , for ^{39}K is shown in figure 3. The relaxation rate increases with increasing temperature. The spin–lattice relaxation time is $T_1 = 32.22$ ms at room temperature. The relaxation rate for the ^{39}K nucleus exhibits a remarkable change near 360 K. The change in the curve of T_1^{-1} near 360 K corresponds to the phase transition. The T_1^{-1} data for the ^{39}K nucleus can be described with the following equation [18, 19]:

$$T_1^{-1} = \alpha T^k + \beta \quad \text{below } T_c \quad (3)$$

with $\alpha = 1.60 \times 10^{-4} \text{ s}^{-1} \text{ K}^{-2}$, $\beta = 18.14 \text{ s}^{-1}$, and $k = 1.9$. The relaxation rate for ^{39}K in $\text{KAl}(\text{SO}_4)_2 \cdot 12\text{H}_2\text{O}$ crystals is proportional to T^2 , as shown by the solid curve in figure 3.

The natural abundance of the ^{27}Al ($I = 5/2$) nucleus is 100%, and the NMR spectrum of ^{27}Al is expected to consist of a central line and four satellite resonance lines. However, the NMR spectrum of ^{27}Al in $\text{KAl}(\text{SO}_4)_2 \cdot 12\text{H}_2\text{O}$ has only one line. The presence of only

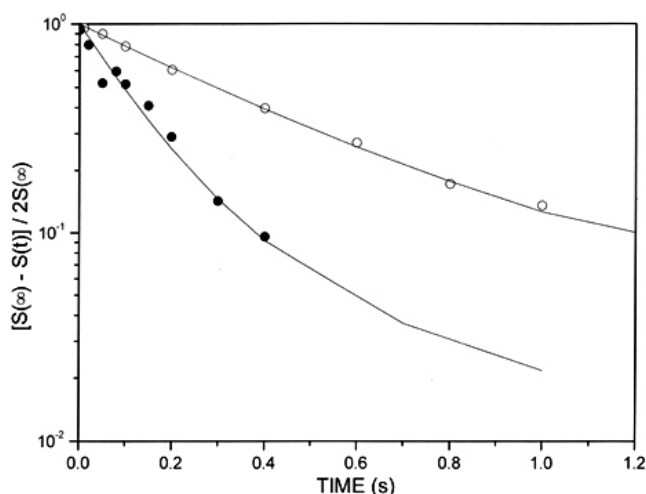


Figure 4. The inversion recovery behaviours of ^{27}Al as a function of delay time at 260 K (●) and 320 K (○). The solid curve is fitted with the function in equation (4).

one ^{27}Al resonance line indicates that the electric quadrupole moments of the ^{27}Al nucleus cause no perturbation of the six nuclear Zeeman levels. This result is consistent with the cubic structure of $\text{KAl}(\text{SO}_4)_2 \cdot 12\text{H}_2\text{O}$ [7]. The ^{27}Al spin–lattice relaxation time was measured in the temperature range 160–400 K at a frequency of 104.23 MHz. The recovery traces of the magnetization of the crystal were measured at several different temperatures. The magnetization recovery of ^{27}Al does not follow a single exponential, but can be represented by a linear combination of three exponential functions, as shown in figure 4 [20, 21]:

$$[S(\infty) - S(t)]/2S(\infty) = [9 \exp(-Wt) + 56 \exp(-6Wt) + 250 \exp(-15Wt)]/315 \quad (4)$$

where $S(t)$ is the nuclear magnetization at time t after saturation, and $2W$ is the inverse spin–lattice relaxation time, T_1^{-1} . The spin–lattice relaxation processes of ^{27}Al at 260 and 320 K are shown in figure 4 as the time evolutions of the resonance spectra with respect to the delay time, and were obtained with the inversion recovery method. The inversion recovery traces of ^{27}Al do not follow a single exponential. The temperature dependence of the spin–lattice relaxation rate, T_1^{-1} , for ^{27}Al in this single crystal is very strong, as shown in figure 5. The ^{27}Al spin–lattice relaxation times are $T_1 = 162$ ms at 200 K and $T_1 = 1784$ ms at 300 K. The relaxation rate for the ^{27}Al nucleus exhibits a remarkable change near 360 K. The relaxation rate, T_1^{-1} , decreases with increasing temperature below 360 K, but slowly increases with increasing temperature above 360 K. The discontinuity in the curve of T_1^{-1} near 360 K corresponds to the first-order phase transition. The relaxation time at the melting point for ^{27}Al is 50.8 ms. The line-width on both sides of the melting point is very narrow. The temperature dependence of the T_1^{-1} data for the ^{27}Al nucleus below 360 K can be fitted with the following function [18, 19]:

$$T_1^{-1} = \gamma T^k + \delta \quad \text{below } T_c \quad (5)$$

where $\gamma = 1.28 \times 10^{18} \text{ s}^{-1} \text{ K}^{-7}$, $\delta = 0.21 \text{ s}^{-1}$, and $k = 7.2$. The temperature dependence of the relaxation rate T_1^{-1} of ^{27}Al in $\text{KAl}(\text{SO}_4)_2 \cdot 12\text{H}_2\text{O}$ between 160 and 360 K was found to be in very good agreement with the law $T_1^{-1} \propto T^7$ below T_c , indicating that the contribution of the higher-order process below T_c is proportional to T^7 . The spin–lattice relaxation of the ^{27}Al nucleus thus occurs via phonon–magnon coupling, which for a Raman relaxation process

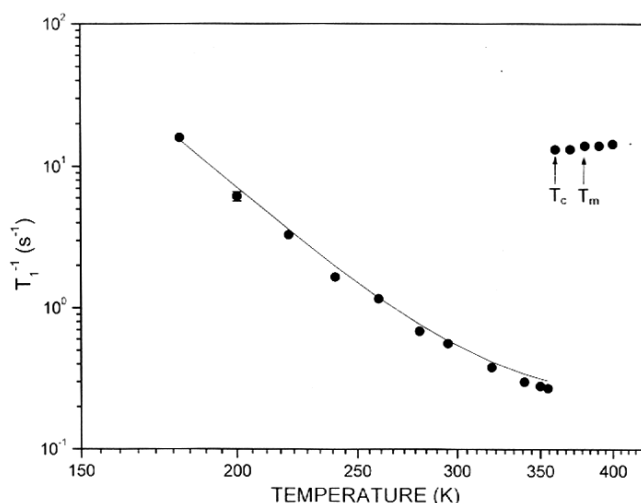


Figure 5. Temperature dependence of the spin–lattice relaxation rate, T_1^{-1} , of ^{27}Al nuclei in a $\text{KAl}(\text{SO}_4)_2 \cdot 12\text{H}_2\text{O}$ single crystal.

results in a T^7 dependence [22]. This result for temperatures below T_c is in agreement with observations for $\text{CuCl}_2 \cdot 2\text{H}_2\text{O}$ [23].

The interaction of the nuclear quadrupole moment with lattice vibrations is a vital relaxation mechanism for nuclear spin with $I \geq 1$ in many crystals. The coupling can generally be written as a spin–lattice Hamiltonian [18]:

$$H = \sum F^{(q)} A^{(q)} \quad (6)$$

where $F^{(q)}$ and $A^{(q)}$ are the lattice and spin operators, respectively, of order q . The lattice operators $F^{(q)}$ (from this point onwards, we omit the index q for brevity) can be expanded as a function of the stress tensor σ :

$$F = F_0 + F_1\sigma + F_2\sigma^2 + F_3\sigma^3 + \dots \quad (7)$$

At temperatures far below the melting temperature of the crystal, we can expect the thermal stress to be small, so only the first few terms of equation (7) are important. The term $F_1\sigma$ represents the absorption or emission of a single phonon (direct process). The next term, $F_2\sigma^2$, indicates the emission or absorption of two phonons or the absorption of one phonon followed by the emission of another one (Raman process). In the direct process, the spin–lattice relaxation rate, T_1^{-1} , is proportional to the square of the frequency ω_0 and to the absolute temperature T for $k_B T / \hbar \omega_0 \gg 1$. In contrast, the Raman process results at high temperatures in a relaxation rate proportional to T^2 . It should be noted that the direct process and the Raman process are both first-order processes within perturbation theory, with perturbing Hamiltonians $F_1\sigma$ and $F_2\sigma^2$ respectively. It has also been suggested that a second-order contribution to the relaxation rate might result from interference between the spin–lattice term $F_1\sigma$ and the anharmonic term $F_3\sigma^3$ in the lattice energy, which is responsible for thermal conductivity. In the framework of the above theory, the spin–lattice relaxation rate is proportional to the absolute temperature T^4 for $k_B T / \hbar \omega_0 \ll 1$. Interference between terms of higher order either in the spin–lattice coupling $F_m\sigma^m$ or in the lattice energy $G_m\sigma^m$ can be seen to lead to smaller contributions.

The relaxation rate for the ^{39}K nucleus is proportional to T^2 , as shown in figure 3, whereas the temperature dependence of the relaxation rate for ^{27}Al is proportional to T^7 below T_c , as

shown by the solid curve in figure 5. Thus, based on the above theory and the experimental results, the relaxation behaviours of ^{39}K and ^{27}Al nuclei in $\text{KAl}(\text{SO}_4)_2 \cdot 12\text{H}_2\text{O}$ single crystals are explained by Raman process. In studies of molecular motion in relation to the experimental relaxation rate, it is important to know whether the relaxation rate is located on the slow side of the minimum or on the fast side of the minimum as a function of the inverse temperature. The general behaviour of the spin–lattice relaxation rate for random motions of the Arrhenius type with a correlation time τ_c can be described in terms of regions of fast and slow motion as follows:

$$\begin{aligned} \omega_0 \tau_c \ll 1, & \quad T_1^{-1} \sim \exp[E_a/RT] && \text{(fast motion)} \\ \omega_0 \tau_c \gg 1, & \quad T_1^{-1} \sim \omega_0^{-2} \exp[-E_a/RT] && \text{(slow motion)} \end{aligned} \quad (8)$$

where ω_0 is the Larmor frequency and E_a is the activation energy. In the case of ^{39}K nuclei, the spin–lattice relaxation rate is in the slow motion region below and above T_c . The spin–lattice relaxation rate of ^{27}Al nucleus is in the fast motion region below T_c , while above T_c it is in the slow motion region.

4. Discussion and conclusion

The phase transition of the $\text{KAl}(\text{SO}_4)_2 \cdot 12\text{H}_2\text{O}$ crystal was investigated by observing the relaxation processes of its ^{39}K and ^{27}Al nuclei. The relaxation rate for the ^{39}K nucleus was found to increase with increasing temperature, and is proportional to T^2 . These results are consistent with the T^2 reported in the ^{39}K nuclei in KHSO_4 and $\text{K}_3\text{H}(\text{SO}_4)_2$ crystals [24]. For the ^{27}Al nucleus, the relaxation rate abruptly decreases below T_c as the temperature is increased, and exhibits a remarkable change above 360 K. The jumps in the ^{39}K and ^{27}Al spin–lattice relaxation rates near 360 K indicate the phase transition of the crystal. We conclude that the abrupt change in T_1^{-1} at T_c is a result of a first-order phase transition. The spin–lattice relaxation time T_1^{-1} for the proton resonance in $\text{KAl}(\text{SO}_4)_2 \cdot 12\text{H}_2\text{O}$ reported by Bloembergen [12] could not be compared to our present results. They did not study the behaviour for T_1^{-1} of the ^1H nucleus near the phase transition temperature, 360 K. The relaxation rates for the ^{39}K and ^{27}Al nuclei can be described using $T_1^{-1} \propto T^2$ and $T_1^{-1} \propto T^7$ respectively. The temperature dependence of the ^{39}K relaxation rate is in accordance with the Raman process, and the ^{27}Al spin–lattice relaxation rate varies with T^7 for $T < T_c$, indicating that three-magnon processes are likely to be responsible for the relaxation of ^{27}Al . Thus for the ^{39}K and ^{27}Al nucleus, the Raman process is more effective for nuclear magnetic relaxation than the direct process is, with $k = 2$ and 7 in the low temperature limit. Our conclusion from the spin–lattice relaxation rates that the phase transition occurs at 360 K agrees with the phase transition temperature identified using DSC.

Acknowledgment

This work was supported by grant No. R04-2003-000-10040-0 from the Basic Research Program of the Korea Science & Engineering Foundation.

References

- [1] Bolanz G and Schafer O 1986 *J. Cryst. Growth* **78** 545
- [2] Sunagawa I, Tsukamoto K, Maiwa K and Onuma K 1995 *Prog. Cryst. Growth Charact.* **30** 153
- [3] Kim S, Myerson A S and Kohl M 1997 *J. Cryst. Growth* **181** 6
- [4] Tolochko N K, Yanusov V A, Myal'dun A Z and Yadroytsev I A 1999 *Crystallogr. Rep.* **44** 1061

-
- [5] Klapper H, Becker R A, Schmiemann D and Faber A 2002 *Cryst. Res. Technol.* **37** 747
- [6] Larson A C and Cromer D T 1967 *Acta Crystallogr.* **22** 793
- [7] Haussuhl S and Buchen H 1986 *Solid State Commun.* **60** 729
- [8] Malekfar R and Sherman W F 1991 *J. Mol. Struct.* **247** 343
- [9] Gronvold F and Meisingset K K 1982 *J. Chem. Thermodyn.* **14** 1083
- [10] Burns G 1960 *J. Chem. Phys.* **32** 1585
- [11] Pake G E 1948 *J. Chem. Phys.* **16** 327
- [12] Bloembergen N 1961 *Nuclear Magnetic Relaxation* (New York: Benjamin)
- [13] Oldfield E, Timken H K C, Montez B and Ramachandran R 1985 *Nature* **318** 163
- [14] Bennema P 1967 *J. Cryst. Growth* **1** 287
- [15] Mullin J W and Garside J 1967 *Trans. Inst. Chem. Eng.* **45** T285
- [16] Denk E G and Botsaris G D 1970 *J. Cryst. Growth* **6** 241
- [17] Igarashi M, Kitagawa H, Takahashi S, Yoshizaki R and Abe Y 1992 *Z. Naturf. a* **47** 313
- [18] Abragam A 1961 *The Principles of Nuclear Magnetism* (Oxford: Oxford University Press)
- [19] Turov E A and Petrov M P 1972 *Nuclear Magnetic Resonance in Ferro- and Antiferromagnets* (New York: Halstead Press)
- [20] Simmons W W, O'Sullivan W J and Robinson W A 1962 *Phys. Rev.* **127** 1168
- [21] Narath A 1967 *Phys. Rev.* **162** 320
- [22] Pincus P and Winter J 1961 *Phys. Rev. Lett.* **7** 269
- [23] Poulis N J, Hardeman G E G and Lugt W V 1956 *Physica* **22** 49
- [24] Lim A R, Jung W K and Han T J 2004 *Solid State Commun.* **130** 481